
OPTIMIZED AUXILIARY PARTICLE FILTERS

Nicola Branchini
School of Informatics
University of Edinburgh
nbranchini17@gmail.com

Víctor Elvira
School of Mathematics
University of Edinburgh
victor.elvira@ed.ac.uk

May 25, 2022

ABSTRACT

Auxiliary particle filters (APFs) are a class of sequential Monte Carlo (SMC) methods for Bayesian inference in state-space models. In their original derivation, APFs operate in an extended space using an auxiliary variable to improve the inference. Later works have re-interpreted APFs from a multiple importance sampling perspective. In this perspective, the proposal is a mixture composed of kernels and weights that are selected by taking into account the latest observation.

In this work, we further exploit this perspective by proposing an online, flexible framework for APFs that adapts the mixture proposal by convex optimization and allows for a controllable computational complexity. We minimize the discrepancy between the proposal and the filtering distribution at a set of relevant points, which are chosen by leveraging the structure of SMC. We compare our method to state-of-the-art particle filters, showing better performance in challenging and widely used dynamical models.

Keywords Sequential Monte Carlo · Particle Filters · Monte Carlo methods · Convex Optimization

1 Introduction

State-space models (SSMs) allow a mathematical description of complex dynamical systems which are very relevant in computational statistics, machine learning and signal processing, among many other fields [1, 2]. Particle filters (PF) or sequential Monte Carlo methods (SMC) are the *de facto* family of algorithms to perform inference tasks in virtually any SSM, e.g., filtering, prediction, or parameter estimation [3, 4, 5, 6]. PFs have been used extensively for solving complex real-world problems in robotics [7], object tracking [8, 9, 10], image processing [11, 12], financial econometrics [13, 14], and even modelling of spread of infectious diseases [15, 16, 17]. PFs are also used for problems beyond the classical SSM setting. For instance, they have been recently applied in reinforcement learning [18, 19, 20], generative modelling [21, 22, 23], and more generally for approximate Bayesian inference in large probabilistic models [24, 25, 26, 27].

PFs are Monte Carlo methods [28] that approximate probability density functions (pdfs) of interest with M particles. The *bootstrap PF* (BPF) [29] is the most popular algorithm, because of its simplicity and reasonable performance in several settings. However, alternatives are needed for challenging applications that require models with complex posterior distributions. Most notably, the *auxiliary PF* (APF) [30] was designed to deal with very informative observations. Since it was proposed, the APF has been re-interpreted under different perspectives [31, 32]. However, the APF still presents an insufficient behavior in many applications of interest, and the development of better PFs is crucial to address new challenges in sequential learning.

In this paper, we develop a flexible framework named *optimized APF* (OAPF) for accurate inference in SSMs. The OAPF framework is motivated by recent advances in multiple importance sampling (MIS) [33, 34, 35], implementing within PF a mixture proposal sampling and a weighting scheme that allows for a variance reduction in the importance weights, the key aim in SMC methods [36].

The structure of the paper is as follows. In Section 2, we review SSMs and give a brief overview on PFs. In Section 3, we derive our OAPF framework, discussing the design choices and providing a theoretical analysis of its estimators. In

Section 5, we show improved results against common particle filters and the recent improved APF [37] in challenging and widely used nonlinear state-space models such as a stochastic Lorenz 63 model and a multivariate stochastic volatility model. We conclude the paper in Section 6 with some final remarks.

Contributions. (1) We develop the optimized auxiliary particle filter (OAPF) framework, which encompasses other particle filters as special cases and allows the development of new algorithms with improved estimators. Our framework has a flexible mixture proposal distribution which appears in the importance weights, provably reducing their variance.

(2) We prove that the resulting marginal likelihood estimators are unbiased and consistent, generalizing the APF estimator in [38]. The marginal likelihood is a key quantity in PF, directly related to the variance of the importance weights, and needed for model selection and parameter estimation.

(3) We propose strategies to select kernels and mixture weights in the proposal. The mixture weights are optimized by matching proposal and posterior at a set of relevant points. Crucially, this allows us to find mixture weights as a solution to a *convex* optimization problem. Therefore, our strategy allows for optimizing the proposal in very generic models (transition and observation pdfs), while avoiding black-box non-convex optimization methods that are common in for instance in variational inference [39, 40, 41]. Further, we allow for a flexible choice of the number of kernels, detaching this choice from the number of particles unlike previous works (see for instance [42]).

(4) We propose specific implementations of our framework and show their effectiveness with widely used state-space models. We compare to BPF, APF and to the improved APF (IAPF) [37], a recent algorithm which provides the state-of-the-art in terms of importance weight variance. We show evidence for better estimates in OAPF with similar computational complexity.

2 Background

2.1 State-Space Models and Particle Filtering

State-space models (SSM) describe the temporal evolution of a system in a probabilistic manner. They are composed of a stochastic discrete-time Markovian process of a (potentially multivariate) *hidden state* $\{\mathbf{x}_t\}_{t \geq 1}$, which can only be observed via corresponding noisy measurements $\{\mathbf{y}_t\}_{t \geq 1}$. SSMs are fully specified by a prior probability density function (pdf), $p(\mathbf{x}_0)$, and by the *transition* and *observation* kernels, $f(\mathbf{x}_t|\mathbf{x}_{t-1})$ and $g(\mathbf{y}_t|\mathbf{x}_t)$, respectively, defined for $t \geq 1$. In these models, the *filtering* task consists in the sequential estimation of the filtering density $p(\mathbf{x}_t|\mathbf{y}_{1:t})$, as well as expectations of the form

$$I(h_t) \triangleq \mathbb{E}_{p(\mathbf{x}_t|\mathbf{y}_{1:t})}[h_t(\mathbf{x}_t)] = \int h_t(\mathbf{x}_t) p(\mathbf{x}_t|\mathbf{y}_{1:t}) d\mathbf{x}_t, \quad (1)$$

for (integrable) functions of interest. For most SSMs of interests, the filtering pdf is intractable and one needs to resort to approximate inference. In this context, particle filters (PFs) are the most popular inferential methods, approximating the filtering pdf with a set of random particles (Monte Carlo samples). PFs are a sequential implementation of importance sampling (IS), generating at each time step M particles $\{\mathbf{x}_t^{(m)}\}_{m=1}^M$ from a proposal pdf $q(\mathbf{x}_t)$ and assigning them normalized importance weights $w_t^{(m)}$. The unnormalized importance weights can be computed by updating the previous weights as

$$\tilde{w}_t^{(m)} = w_{t-1}^{(m)} \frac{g(\mathbf{y}_t|\mathbf{x}_t^{(m)})f(\mathbf{x}_t^{(m)}|\mathbf{x}_{t-1}^{(m)})}{q(\mathbf{x}_t^{(m)}|\mathbf{y}_t, \mathbf{x}_{t-1}^{(m)})}, \quad (2)$$

which can be derived by factorizing the joint proposal in a recursive way $q(\mathbf{x}_{1:t-1}|\mathbf{y}_{1:t})q(\mathbf{x}_t|\mathbf{y}_t, \mathbf{x}_{t-1})$ and targeting $p(\mathbf{x}_{1:t}|\mathbf{y}_{1:t})$ [1]. Therefore, a particle filter maintains a set of normalized weights and particles $\{w_t^{(m)}, \mathbf{x}_t^{(m)}\}_{m=1}^M$ as a representation of the filtering pdf, updating weights at each time step with as in Eq. (2). The most popular choice for $q(\mathbf{x}_t|\mathbf{y}_t, \mathbf{x}_{t-1})$ is $f(\mathbf{x}_t|\mathbf{x}_{t-1})$ and leads to the concrete bootstrap particle filter (BPF) [29]. The advantage of this choice is that the weights in (2) simply become $w_{t-1}^{(m)}g(\mathbf{y}_t|\mathbf{x}_t^{(m)})$. In practice, particle filters suffer from the *weight degeneracy* effect [1], consisting on few normalized weights taking all probability mass (i.e., the posterior is approximated with very few samples). In the BPF, a resampling step is introduced to mitigate this effect (see more details in [43]). In some implementations, the resampling step is performed only when the effective sample size $\text{ESS} = \frac{1}{\sum_{m=1}^M (w_t^{(m)})^2}$ is below some threshold [3, 36, 1].

2.2 Auxiliary Particle Filters

Auxiliary PFs (APFs) were introduced to alleviate some of the limitations of existing PF methods [30]. For instance, it is well known that informative likelihoods often impact negatively the ability of the standard BPF to reconstruct the filtering pdf [36, 44, 45].¹ Intuitively, the reason is that the resampling step at the end of the recursion at time $t - 1$ does not take into account the new observation \mathbf{y}_t . In the standard APF, the resampling step at $t - 1$ is delayed until the new observation \mathbf{y}_t is available. Then the resampling is performed with modified unnormalized weights

$$\tilde{\lambda}_t^{(m)} = w_{t-1}^{(m)} g(\mathbf{y}_t | \boldsymbol{\mu}_t^{(m)}), \quad \lambda_t^{(m)} = \frac{\tilde{\lambda}_t^{(m)}}{\sum_{m=1}^M \tilde{\lambda}_t^{(m)}}, \quad (3)$$

where $\boldsymbol{\mu}_t^{(m)} = \mathbb{E}_{f(\mathbf{x}_t | \mathbf{x}_{t-1}^{(m)})}[\mathbf{x}_t]$. Then the particles are propagated using the transition kernel $f(\mathbf{x}_t | \mathbf{x}_{t-1})$ as in BPF. Finally, the importance weights are chosen as

$$\tilde{w}_{t-1}^{(m)} = \frac{g(\mathbf{y}_t | \mathbf{x}_t^{(m)})}{g(\mathbf{y}_t | \boldsymbol{\mu}_t^{(i^{(m)})})}, \quad (4)$$

where $i^{(m)}$ denotes the index of the ancestor that generates the m -th resampled particle. Intuitively, this can be seen as scaling down the BPF weights, taking into account that particles have been already resampled in large number in regions of high likelihood [42]. A different interpretation of APFs is possible from the multiple importance sampling (MIS) perspective [42]. Note that MIS refers to the different sampling and weighting schemes that are possible in the presence of multiple proposals in IS [46, 35]. In this perspective, a resampling step followed by a propagation step is considered to be simply a single sampling step from a mixture pdf. Moreover, it shows that the mixture weights and importance weights can be derived by using approximations that in some models are too loose, which explains the poor behavior of APF in many settings. The improved APF (IAPF) overcomes these approximations at the expense of increasing the computational complexity of calculating $\lambda_t^{(m)}$ [37]. The MIS perspective is also related to auxiliary marginal particle filters (AMPF) [32], where a similar importance weight is derived. The AMPF interpret that the inference is performed in the marginal space of \mathbf{x}_t (marginalizing the auxiliary variable), which guarantees to reduce the variance of the importance weights (it is a Rao-Blackwellization that can be proved by the variance decomposition lemma [32]).

3 Optimized Auxiliary Particle Filters

3.1 The OAPF Framework

In this section, we present our new framework for *optimized auxiliary particle filters* (OAPFs). The OAPF framework builds upon the MIS perspective, considering a generic mixture as proposal where all samples are (independently) simulated from. More precisely, we consider the generic mixture proposal at each time step t as

$$\psi_t(\mathbf{x}_t) = \sum_{k=1}^K \lambda_t^{(k)} q_t^{(k)}(\mathbf{x}_t), \quad (5)$$

with associated mixture weights $\lambda_t^{(k)}$. To the best of our knowledge, the OAPF is the first method to detach the choice of K from the number of samples M (i.e., $K \neq M$ in the general case).

The OAPF framework is described in Algorithm 1. The method starts by simulating M samples from the prior pdf, and then at each time t , it consists of the three following stages: (a) optimization, (b) sampling, and (c) weighting steps. Note that this structure keeps also some ties with adaptive IS (AIS) algorithms [47]. First, the optimization step adapts the mixture proposal of Eq. (5). This procedure is discussed in detail in the next Section. Second, the new M particles are simulated from the mixture proposal. Third, the importance weights are calculated as in Eq. (7). Note that, although unusual in PF, they follow a standard structure in MIS, with the whole mixture in the denominator. It is worth remarking that the numerator does not evaluate the true filtering pdf but only an (unnormalized) approximation. However, the importance weights are still *proper* [48], as we show below.

Note that the importance weights play a crucial role both in the estimators of generic moments of the approximate distributions and also in the behavior of the PF for the next time step. Hence, reducing the variance of the importance weights is the ultimate goal in PF. Since this variance depends on the discrepancy between the proposal and target pdfs

¹Informally, an informative likelihood refers to a peaky likelihood that heavily influences the shape of the posterior.

Algorithm 1: Optimized Auxiliary Particle Filter**Input:** prior, transition, and observation pdfs $p(\mathbf{x}_0)$, $f(\mathbf{x}_t|\mathbf{x}_{t-1})$, $g(\mathbf{y}_t|\mathbf{x}_t)$, and sequence of observations $\mathbf{y}_{1:T}$ **Output:** set of weighted samples for each time step $\{\mathbf{x}_t^{(m)}, \tilde{w}_t^{(m)}\}_{m=1}^{M,T}$ 1 Draw M samples from prior: $\mathbf{x}_0^{(m)} \sim p(\mathbf{x}_0)$ and set $w_0^{(m)} = 1/M$;2 **foreach** $t = 1, \dots, T$ **do**3 (a) *optimization step*: optimize the mixture proposal by selecting K kernels $q_t^{(k)}$ and choosing their associated mixture weight $\lambda_t^{(k)}$ that compose the mixture proposal ψ_t (see Section 3.2)4 (b) *sampling step*: simulate M particles $\mathbf{x}_t^{(m)}$ from the proposal as

$$\mathbf{x}_t^{(m)} \sim \psi_t(\mathbf{x}_t) \quad (6)$$

5 (c) *weighting step*: calculate new importance weights as:

$$\tilde{w}_t^{(m)} = \frac{g(\mathbf{y}_t|\mathbf{x}_t^{(m)}) \sum_{i=1}^M w_{t-1}^{(i)} f(\mathbf{x}_t^{(m)}|\mathbf{x}_{t-1}^{(i)})}{\sum_{k=1}^K \lambda_t^{(k)} q_t^{(k)}(\mathbf{x}_t^{(m)})} \quad (7)$$

6 **end**

[49, 50] the benefit of considering a mixture proposal in Eq. 5 and for the importance weights in Eq. (7) is twofold. First, mixtures are a flexible way to approximate a large collection of pdfs (see for instance [51, 52, 53]). Second, while PFs work implicitly with mixture proposal, only few of them use them in the denominator of the importance weights [32, 37, 42]. Placing the whole mixture in the denominator, as we do in OAPF, is known to reduce variance in MIS [35], even yielding to zero-variance importance weights in the case of perfect matching between proposal and target pdfs.

In OAPF, the standard IS estimators can be built. More precisely, moments of the filtering pdf as in Eq. (1) can be approximated by the self-normalized IS (SNIS) estimator as

$$\hat{I}(h_t) = \sum_{m=1}^M w_t^{(m)} h_t(\mathbf{x}_t^{(m)}), \quad (8)$$

where $w_t^{(m)} = \frac{\tilde{w}_t^{(m)}}{\sum_{j=1}^M \tilde{w}_t^{(j)}}$ are the normalized weights. Finally, the weights of OAPF can be used to build an unbiased estimator of $p(\mathbf{y}_{1:t})$, which is crucial for many statistical tasks such as model selection [54, 55, 56]. The OAPF estimator of the partial normalizing constant at time t , $p(\mathbf{y}_t|\mathbf{y}_{1:t-1})$, is given by

$$\hat{p}(\mathbf{y}_t|\mathbf{y}_{1:t-1}) \triangleq \frac{1}{M} \sum_{m=1}^M \tilde{w}_t^{(m)}. \quad (9)$$

Since the marginal likelihood admits a decomposition as $p(\mathbf{y}_{1:T}) = p(\mathbf{y}_1) \prod_{t=2}^T p(\mathbf{y}_t|\mathbf{y}_{1:t-1})$, then we can build the OAPF estimator as

$$\hat{p}(\mathbf{y}_{1:T}) \triangleq \hat{p}(\mathbf{y}_1) \prod_{t=2}^T \hat{p}(\mathbf{y}_t|\mathbf{y}_{1:t-1}). \quad (10)$$

The functional form of the OAPF estimator is similar to other PFs and can be justified by standard IS arguments, but the computation of the importance weights $\tilde{w}_t^{(m)}$ differs from other methods as discussed above. In the following, we prove that the estimator $\hat{p}(\mathbf{y}_{1:T})$ is unbiased and consistent, which turns the SNIS estimator of Eq. (8) consistent.

Theorem 1 *For any set of mixture proposals $\{\psi(\mathbf{x}_t)\}_{t=1}^T$ fulfilling standard regularity conditions in IS, the normalizing constant estimator in Eq. (10) is unbiased and consistent, i.e., $\mathbb{E}[\hat{p}(\mathbf{y}_{1:T})] = p(\mathbf{y}_{1:T})$ and $\lim_{M \rightarrow \infty} \hat{p}(\mathbf{y}_{1:T}) = p(\mathbf{y}_{1:T})$ a.s. for any $T \in \mathbb{R}^+$.*

Proof: The proof is presented in the supplementary material as well as a description of the regularity conditions. \square

Note that the consistency of the SNIS estimator in Eq. (8) is also guaranteed by standard IS arguments (we complete this discussion in the supplement).

Finally, note that the minimization of the variance of the normalizing constant is equivalent to minimizing the variance of the importance weights \tilde{w}_t [57, 36]. The OAPF explicitly aims at reducing this variance by minimizing the mismatch

between the target pdf and the mixture proposal. In the supplement, we also present a proof showing that the variance the OAPF weights in Eq. (7) is always less than those of APF in Eq. (4), when $K = M$ and the mixture weights are the same.

3.2 Selection of the Mixture Weights

In this section we discuss an approach to select the weights of the mixture proposal ψ_t . The ultimate goal is to select them so that the proposal is a good approximation of the approximate filtering posterior. To achieve this, we impose these two distributions to be equal at a set of E *evaluation points* $\{\mathbf{z}_t^{(e)}\}_{e=1}^E$. We will show that this approach is flexible and brings several advantages. For simplicity, we start considering the case with $K = E$, where the evaluation points are the centers of the K kernels $q^{(k)}$ in the proposal (5), i.e., $\{\mathbf{z}_t^{(e)}\}_{e=1}^E = \{\boldsymbol{\mu}_t^{(k)}\}_{k=1}^K$. More precisely, the K kernels could be chosen as a subset K elements from the set of M transition kernels (from the previous M particles). Note that APF and improved APF [42] also recommend the use of the center of the transition kernel. Alternatively, we could also use “optimal” SMC kernels [36] which are defined via the intractable function $p(\mathbf{x}_t|\mathbf{x}_{t-1}, \mathbf{y}_t)$. Our framework allows for generic choices so these restrictions are not necessary. We continue this section in a generic setting, expanding this discussion in Section 3.3.

Now that we have chosen the K mixture kernels and the E evaluation points, we can satisfy the condition previously mentioned and build a *linear* system of E equations as:

$$\sum_{k=1}^K \lambda_t^{(k)} q_t^{(k)}(\mathbf{z}_t^{(e)}) = g(\mathbf{y}_t|\mathbf{z}_t^{(e)}) \sum_{m=1}^M w_{t-1}^{(m)} f(\mathbf{z}_t^{(e)}|\mathbf{x}_{t-1}^{(m)}), \quad e = 1, \dots, E, \quad (11)$$

where the K mixture weights $\lambda_t^{(k)}$ are unknown at each time t . For a unique solution to exist is necessary that $K = E$, but in general we do not need to restrict to this case. Below, we show how to turn this problem into a (constrained) *convex* optimization problem. Let us first define the following vectors:

$$\begin{aligned} \boldsymbol{\lambda} &\triangleq (\lambda_t^{(1)}, \lambda_t^{(2)}, \dots, \lambda_t^{(K)})^\top, \\ \mathbf{w} &\triangleq (w_{t-1}^{(1)}, w_{t-1}^{(2)}, \dots, w_{t-1}^{(M)})^\top, \\ \mathbf{f}^{(e)} &\triangleq (f(\mathbf{z}_t^{(e)}|\mathbf{x}_{t-1}^{(1)}), \dots, f(\mathbf{z}_t^{(e)}|\mathbf{x}_{t-1}^{(M)}))^\top, \\ \mathbf{q}^{(e)} &\triangleq (q^{(1)}(\mathbf{z}_t^{(e)}), \dots, q^{(K)}(\mathbf{z}_t^{(e)}))^\top. \end{aligned}$$

Then, we can re-write Eq. (11) as

$$\mathbf{q}^{(e)\top} \boldsymbol{\lambda} = \underbrace{g(\mathbf{y}_t|\mathbf{z}_t^{(e)}) \odot \mathbf{w}^\top \mathbf{f}^{(e)}}_{\tilde{\boldsymbol{\pi}}^{(e)}}, \quad (12)$$

for $e = 1, \dots, E$, where \odot is elementwise multiplication and defining additionally the right-hand side to be $\tilde{\boldsymbol{\pi}}^{(e)}$. More compactly, the above can be re-expressed in matrix form as:

$$\overbrace{\begin{bmatrix} \text{---} & \mathbf{q}^{(1)\top} & \text{---} \\ \vdots & \vdots & \vdots \\ \text{---} & \mathbf{q}^{(E)\top} & \text{---} \end{bmatrix}}^{E \times K} \overbrace{\begin{bmatrix} \lambda \\ \vdots \\ \lambda \end{bmatrix}}^{K \times 1} = \overbrace{\begin{bmatrix} \text{---} & g(\mathbf{y}_t|\mathbf{z}_t^{(1)}) \odot \mathbf{f}^{(1)\top} & \text{---} \\ \vdots & \vdots & \vdots \\ \text{---} & g(\mathbf{y}_t|\mathbf{z}_t^{(M)}) \odot \mathbf{f}^{(E)\top} & \text{---} \end{bmatrix}}^{E \times M} \overbrace{\begin{bmatrix} \mathbf{w} \\ \vdots \\ \mathbf{w} \end{bmatrix}}^{M \times 1}, \quad (13)$$

defining \mathbf{Q} as the $E \times K$ matrix on the left-hand side of (13) and $\tilde{\pi}$ as the resulting $E \times 1$ vector on the right-hand side. We now define a generic constrained optimization problem as for the mixture weights as:

$$\lambda^* = \arg \min_{\lambda} \mathcal{L}(\mathbf{Q}\lambda, \tilde{\pi}), \quad (14)$$

where $\mathcal{L}(\cdot)$ a generic loss function. The optimization will be constrained since λ will be used for resampling, and therefore needs to have non-negative elements.² In the next Section, we present a possible strategy to implement $\mathcal{L}(\cdot)$ and solve the optimization problem.

Optimization via Non-Negative Least Squares (NNLS) The previous problem can be encoded as a non-negative least squares problem by taking the squared distance of the pdfs at the E evaluation points $\{\mathbf{z}_t^{(e)}\}_{e=1}^E$. Taking squared differences between left-hand side and right-hand side of (13) leads to:

$$\begin{aligned} \lambda^* &= \arg \min_{\lambda} \|\mathbf{Q}\lambda - \tilde{\pi}\|_2^2 \\ &\text{subject to : } \lambda \in \mathbb{R}_{\geq 0}^K. \end{aligned}$$

This problem is a (constrained) quadratic program. Therefore, it is convex and the non-negativity constraints form a convex feasible set. When \mathbf{Q} has full column rank, then there is a unique solution. Theoretical results on NNLS have shown that, especially when the dimension of \mathbf{Q} is large (large K and E in our case), the solutions tend to be very sparse [58, 59, 60]. The optimization problem can be solved by the widely used algorithm in [61] (see also a faster version in [62]), as well as by concurrent work on exact sparse NNLS [63] and even strong GPU accelerations could be exploited [64, 65]

3.3 Selection of Kernels, Evaluation Points and Computational Complexity

The computational complexity of the strategy of the NNLS algorithm is worst-case $\mathcal{O}(\max(K, E)^2 \cdot \min(K, E) + MK)$ (calculation of mixture weights and weighting step) runtime, and $\mathcal{O}(KE)$ space to store the matrix \mathbf{Q} , thus depending on the choices of K and E . The selection of the number of kernels K depends on the shape of the target pdf but also in the positions of the mixture kernels. In our experiments, we will take a simple approach by inheriting the standard transition kernels used for instance in BPF or APF. This allows to reduce K and E w.r.t. M in some cases, as we show in the numerical experiments. As a general guideline, a good starting point is setting $K = E$ and choosing the evaluation points as the center of the kernels, retaining those kernels associated with the E greatest values of the approximate filtering pdf. More strategies could be explored in further work.

Finally, we recall that in NNLS, the solutions are in general sparse, as explained in Section 3.2, so the *effective* number of kernels (i.e., those with $\lambda_t^{(k)} > 0$) is often much less than K [60]. This greatly simplifies the mixture sampling stage and also reduces the runtime of the weighting step in Eq. (7). Note that the weighting step could be reduced from $\mathcal{O}(MK)$ to $\mathcal{O}(M \log K)$ with dual-tree methods [32].

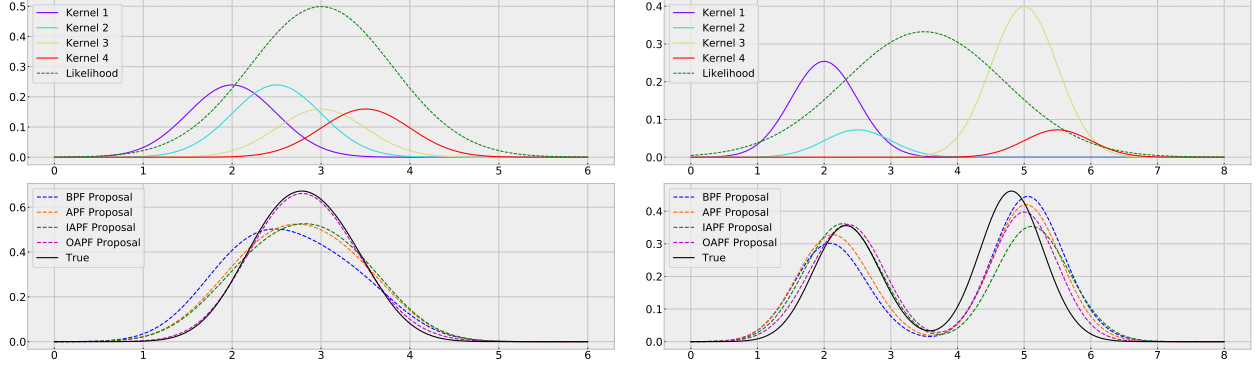
4 Related Work

The OAPF follows a different approach w.r.t. most papers in the literature by interpreting the M samples to be simulated from a mixture proposal, and hence explicitly including that proposal in the denominator. This perspective is connected to the auxiliary marginal PF (AMPF) [32] and improved APF (IAPF) [37] algorithms, and is supported by recent advances in MIS [35] (see also the discussion of the variance reduction in [32]), and it also links with the re-interpretation of BPF and APF [42]. The selection of the mixture weights is also linked with other works. For instance, a flexible framework named *twisted* APFs is developed in [66], where APFs are interpreted as a special case of changing the distribution targeted in IS (this interpretation appeared first in [44, 36]. In this method, the computation is done in an offline fashion (see an extension of this line in [67]). In [68], they develop a PF framework with a different approach, preemptively moving a subset of particles to a region of high likelihood with gradient methods. In [69], the method adapts a mixture of kernels in a more generic setup (sequential Monte Carlo samplers), focussing in the choice of kernels. A novel APF is proposed in [70], propagating the particles associated with kernels that are placed high likelihood regions. Their approach could also be combined with our proposed OAPF method.

5 Experiments

We compare OAPF with BPF, APF as well as the recent improved APF (IAPF) [37], which also uses a mixture in the denominator of the importance weights and can be seen as a special case in our framework. The IAPF strictly improves

²The resulting values can be normalized afterwards so they parametrize the mixture proposal in Eq. (5).



(a) In this first example we choose a unimodal posterior. OAPF substantially outperforms the other algorithms.

(b) OAPF is the only algorithm who can match well *both* modes simultaneously with this multimodal posterior.

Figure 1: Experiment 1 (Toy Example.) In this experiment we show that OAPF proposals are closer to true posteriors compared to its competitors. We calculated χ^2 -divergence for these examples in Table 1. Note that here OAPF uses transition kernels for the proposal and their centers as evaluation points. We provide all parameters for reproducibility in the supplement.

over APF and BPF in most settings [37]. Note that the simple BPF can sometimes perform unexpectedly well, as it is well known in the PF community. We evaluate our framework in 4 sets of experiments (see below).

Our aim is to show the benefits of OAPF in terms of variance of importance weights, which is crucial in particle filters: the weights are used not only for approximating integrals of interest but also for building better particle approximations in the next time steps. Therefore, we choose metrics that are directly connected to the variance of the importance weights: χ^2 -divergence between mixture proposal and filtering pdfs, error in the estimation of the marginal likelihood, and effective sample size (ESS) [1]. The setup of the experiments is as follows:

- **Experiment 1: Toy example.** We show visually that the mixture proposal in OAPF reconstructs the posterior better than its competitors, both with unimodal and multimodal posteriors. Numerically we show an improved χ^2 -divergence between proposal and filtering pdfs, which directly translates into lower variance of importance weights.
- **Experiment 2: Linear dynamical model.** We exploit the closed-form solution of the linear dynamical model, perhaps the most known SSM and widely used for instance in object tracking [1]. This allows an evaluation of the estimators of the marginal likelihood, $p(y_{1:t})$. We show that OAPF reaches better solutions with, while highly reducing the runtime.
- **Experiment 3: Stochastic Lorenz 63 model.** Transitioning to more challenging non-linear non-Gaussian models, we show an improved performance on discretized version of this popular chaotic dynamical system [71], which is used for instance in atmospheric models for weather forecasting [72, 73]. We compare the PFs in terms of the ESS, which is widely used as a proxy for the weight variance when the true normalizing constant is not available (as it is the case here).
- **Experiment 4: Stochastic volatility model.** Finally, we perform inference for a multivariate stochastic volatility model used in related work on APFs [74]. Here, as in Experiment 4, we look at ESS and show improved performance against all other algorithms.

We consider time-series with $T = 100$ time steps, except otherwise stated. We let $d_{\mathbf{x}_t}$ be the dimension of the hidden state, i.e., $\mathbf{x}_t \in \mathbb{R}^{d_{\mathbf{x}_t}}$. In general we use $M = 100$ particles, except for $d_{\mathbf{x}_t} = 10$ where $M = 1000$. Due to the curse of dimensionality [75], a general reduction in performance for all methods is expected as $d_{\mathbf{x}_t}$ grows. For linear dynamical models, we show improved estimates with significantly reduced runtime than all other algorithms, including IAPF. For the more challenging models, we achieve better ESS than the competitors. Note that in those experiments, we set $K = E = M$. However, due to the high sparsity of solutions in OAPF, our effective K is much lower. For $M = 1000$ particles we report an average of 88% sparsity, while for $M = 100$ an average of 65%. All averages, standard errors and boxplots are obtained with 100 independent Monte Carlo runs.³

³The code of all experiments will be made available upon publication.

Table 1: **Experiment 1 (Toy example).** χ^2 -div. between filtering and mixture proposal pdfs in Figure 1.

Method	χ^2 -div. (Fig. 1a)	χ^2 -div. (Fig. 1b)
BPF	0.1662	0.2245
APF	0.0916	0.1633
IAPF	0.0870	0.2402
OAPF	0.0069	0.0819

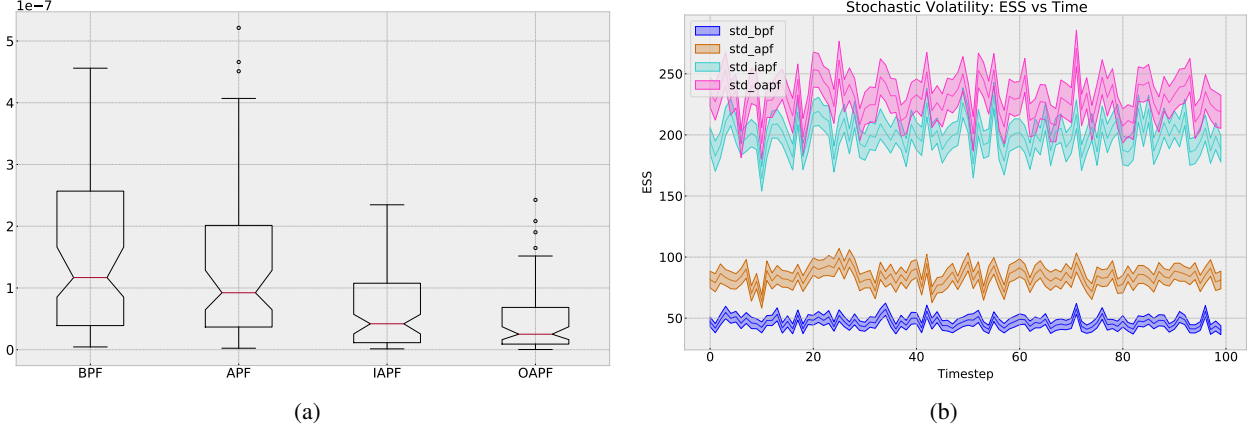


Figure 2: **Experiment 2 (Linear dynamical model)** 2a: boxplot of normalized MSE for (log) marginal likelihood estimates with $d_{\mathbf{x}_t} = 10$. Note that in this experiment, $K = E = 5$ so OAPF runs with greatly reduced runtime. **Experiment 4 (Stochastic volatility)** 2b: ESS over timesteps with $d_{\mathbf{x}_t} = 10$.

1. Toy Example. The main goal of this toy example is to illustrate that the OAPF mixture proposal better reconstructs the filtering pdf. We also measure the χ^2 -divergence between both pdfs. We consider a single iteration of each PF algorithm and build artificial proposals by multiplying a mixture of 4 Gaussians with a Gaussian likelihood. Results from the two experiments with the above setting are shown in Figure 1. We select the means of the transition kernel as evaluation points, and set $K = E = M = 4$. In Figure 1a, we show the results for a unimodal posterior. This setting is advantageous for the IAPF, as transition kernels significantly overlap (see [42] for more details). The likelihood is sufficiently informative, which explains why APF outperforms BPF. Figure 1b shows a more complex multimodal posterior with a more diffused likelihood. Interestingly, we find that IAPF can perform even worse than APF, while our OAPF does not suffer from this issue. Table 1 quantifies (for both settings) the mismatch between mixture proposal and filtering pdfs in terms of χ^2 -divergence, confirming the visual analysis of Fig. 1a.

2. Linear Dynamical Model. The linear dynamical model is arguably the most popular SSM, routinely being the first choice to assess PFs [2, 76, 77]. It has been applied in a wide range of applications (e.g., robotics [1]). This model is particularly useful for validating PFs since it is one of the few models admitting closed-form solutions of the filtering distribution and the normalizing constant (via the celebrated *Kalman filter* [78]). The defining transition and observation equations are standard (see e.g., [1]) and require mainly the selection of observation and transition covariances (we provide more details in the supplement). We used observation covariance is $5\mathbf{I}$ and transition covariance $2.5\mathbf{I}$. This is again a favourable setting for the competitor IAPF because of the wide transition kernel w.r.t. observation kernel. We calculate the normalized mean-squared error (NMSE) between our unbiased estimates of the marginal likelihood $p(\mathbf{y}_{1:t})$ and the true value for $d_{\mathbf{x}_t} \in \{2, 5, 10\}$. We define NSME as mean-squared error divided by true value of $p(\mathbf{y}_{1:t})$. In Figure 2 we show boxplots of NSME for all methods with $d_{\mathbf{x}_t} = 10$. We set $M = 100$ and $M = 1000$. In both cases, the proposed OAPF outperforms all the competitors, while setting a low $K = E = 5$, which is translated into large computational savings. Similar conclusions can be extracted for other choices of the model parameters. In the supplement, we include complementary results for this model with $d_{\mathbf{x}_t} \in \{2, 5\}$.

3. Stochastic Lorenz 63 Model. The Lorenz 63 [71] is a *chaotic* system, since slightly different initial conditions generate extremely different trajectories. Due to this difficulty, this model is often used to evaluate PFs [79, 68]. We consider a discretized version of the state dynamics using an Euler-Maruyama scheme and observations with additive noise. The hidden state is three dimensional $\mathbf{x}_t = [x^{[1]}, x^{[2]}, x^{[3]}]$ and the transition dynamics are defined by the

Table 2: **Experiment 3 (Lorenz)**. $T = 1000$ timesteps, $M = 100$ particles. Averaged ESS and standard errors.

Method	$\Delta t = 0.01$	$\Delta t = 0.008$
BPF	57.7 ± 0.2	58.1 ± 0.2
APF	55.1 ± 0.2	55.2 ± 0.2
IAPF	70.1 ± 0.1	71.0 ± 0.1
OAPF	76.7 ± 0.1	76.4 ± 0.1

Table 3: **Experiment 4 (Stochastic Volatility)**. Note that when $d_{\mathbf{x}_t} = 10$ then $M = 1000$. Averaged ESS and standard errors.

Method	$d_{\mathbf{x}_t} = 2$	$d_{\mathbf{x}_t} = 5$	$d_{\mathbf{x}_t} = 10$
BPF	50.8 ± 0.2	21.2 ± 0.4	46.6 ± 0.5
APF	59.7 ± 0.2	31.9 ± 0.4	83.9 ± 0.6
IAPF	80.5 ± 0.1	49.4 ± 0.5	199.9 ± 1.7
OAPF	92.6 ± 0.1	59.5 ± 0.7	239.5 ± 2.4

differential equations:

$$dx^{[1]} = \sigma(x^{[2]} - x^{[1]})d\tau + dw_{x^{[1]}} \quad (15)$$

$$dx^{[2]} = (\rho x^{[1]} - x^{[3]}x^{[1]} - x^{[2]})d\tau + dw_{x^{[2]}} \quad (16)$$

$$dx^{[3]} = (x^{[1]}x^{[2]} - \beta x^{[3]})d\tau + dw_{x^{[3]}} \quad (17)$$

where τ denotes continuous time, $w_{x^{[1]}}$, $w_{x^{[2]}}$, $w_{x^{[3]}}$ are independent one-dimensional standard Wiener processes and (σ, ρ, β) are parameters of the model. We use the an increment Δt in the discretization, and partially observe the hidden state (only the first dimension) with scalar $y_t \sim \mathcal{N}_{y_t}(x^{(1)}, \sigma_{y_t}^2 = 1)$, using the standard values for (σ, ρ, β) (see supplement). The results of averaged ESS with two different values of $\Delta t \in \{0.01, 0.008\}$ are shown in Table 2. Note that even these small changes in Δt cause very different trajectories, as we also show in the supplement.

4. Stochastic Volatility Model. We perform inference in a multivariate stochastic volatility model (SVM), a type of stochastic process where the variance is a latent variable that follows itself a stochastic process. These are extremely useful models to apply for many tasks in econometrics, e.g., for predicting the volatility of a heteroskedastic sequence such as returns on equity indices or currency exchanges [80]. SVMs are often used to evaluate particle filters [30, 81, 82, 32, 74]. We employ the version in [83], which is also used in related work on APFs [66]. It is defined by the following prior, transition and observation pdfs:

$$p(\mathbf{x}_0) = \mathcal{N}_{\mathbf{x}_0}(\mathbf{m}, \mathbf{U}_0), \quad (18)$$

$$f(\mathbf{x}_t | \mathbf{x}_{t-1}) = \mathcal{N}_{\mathbf{x}_t}(\mathbf{m} + \text{diag}(\phi)(\mathbf{x}_{t-1} - \mathbf{m}), \mathbf{U}), \quad (19)$$

$$g(\mathbf{y}_t | \mathbf{x}_t) = \mathcal{N}_{\mathbf{y}_t}(\mathbf{0}, \exp(\text{diag}(\mathbf{x}_t))). \quad (20)$$

Table 3 shows averaged ESS for $d_{\mathbf{x}_t} = (2, 5, 10)$ while Figure 2b shows the averaged ESS over time for $d_{\mathbf{x}_t} = 10$. The parameters for this experiment are set to $\mathbf{m} = \mathbf{0}$, $\mathbf{U}_0 = \mathbf{I}$, $\mathbf{U} = \mathbf{I}$, $\phi = \mathbf{1}$. For results with additional parameters, see supplementary.

6 Conclusions

In this paper we have proposed OAPF, a flexible framework for particle filtering that uses a generic mixture distribution as a proposal and includes previous methods as special cases. The framework allows for the development of particle filters with improved performance, and we provide a explicit implementation. We have proved the unbiasedness of the OAPF marginal likelihood estimator for any mixture proposal that fulfills standard IS requirements. We also show the effectiveness of OAPF in reducing the variance of the IS estimators. In OAPF, we directly optimize the mixture proposal to the posterior in an online fashion, rather than making specific analytic choices of mixture weights like in AMPF or IAPF. Conversely to most other methods that optimize a proposal (e.g., variational inference), our optimization strategy is convex, directly addresses the ultimate goal of minimizing the variance of the importance weights, and can deal with

any likelihood and transition models all, at the same time, without resorting to black-box, non-convex methods (see for instance [39, 41]). We have shown an improved performance of the proposed implementation of the OAPF across a series of challenging state-space models and metrics, comparing with BPF, APF and the competitive IAPF. Finally, the flexibility and the strong theoretical guarantees of OAPF pave the way for new methodological advances within this framework.

A Supplementary Material

A.1 Theoretical Properties of the OAPF Estimators

The theoretical properties of the estimators OAPF are analyzed from the importance sampling perspective. In the case of the mixture proposals ψ_t , we assume that each time t , the support of ψ_t is a superset of the support of $p(\mathbf{x}_t|\mathbf{y}_{1:t})$, i.e., that $\psi_t(\mathbf{x}_t) > 0$ for all \mathbf{x}_t where $p(\mathbf{x}_t|\mathbf{y}_{1:t}) > 0$. Let us define the *partial* normalizing constants as $Z_t \triangleq p(\mathbf{y}_t|\mathbf{y}_{1:t-1})$, the *joint* normalizing constant as $Z_{1:t} \triangleq p(\mathbf{y}_{1:t})$, and also $Z_{t-h:t} \triangleq p(\mathbf{y}_{t-h:t}|\mathbf{y}_{1:t-h-1})$. In the OAPF framework, we can build estimator of those quantities, e.g., the partial estimator $\hat{Z}_\tau \triangleq \frac{1}{M} \sum_{m=1}^M \tilde{w}_\tau^{(m)}$, the joint estimator $\hat{Z}_{1:t} = \prod_{\tau=1}^t \hat{Z}_\tau$, and also the estimator $\hat{Z}_{t-h:t} = \prod_{\tau=t-h}^t \hat{Z}_\tau$, with and the estimator $\hat{Z}_t \triangleq \frac{1}{M} \sum_{m=1}^M \tilde{w}_t^{(m)}$. We also assume that the estimators of all the partial normalizing constants have finite variance (see for instance [33, 35]). We define the set of weighted samples at time t as $\mathcal{A}_t \triangleq \{\mathbf{x}_t^{(m)}, \tilde{w}_t^{(m)}\}_{m=1}^M$. In order to avoid ambiguities when evaluating pdfs, we define the functions $g(\mathbf{y}_t|\mathbf{x}_t) \triangleq p(\mathbf{y}_t|\mathbf{x}_t)$, $g(\mathbf{y}_t|\mathbf{x}_{t-1}) \triangleq p(\mathbf{y}_t|\mathbf{x}_{t-1})$, $g(\mathbf{y}_t, \mathbf{x}_t|\mathbf{x}_{t-1}) \triangleq p(\mathbf{y}_t, \mathbf{x}_t|\mathbf{x}_{t-1})$ and $g(\mathbf{y}_{t-h:t}, \mathbf{x}_t|\mathbf{x}_{t-1}) \triangleq p(\mathbf{y}_{t-h:t}, \mathbf{x}_t|\mathbf{x}_{t-1})$.

In the following, we show that OAPF provides an unbiased estimator of the normalizing constant $p(\mathbf{y}_{1:t})$, which follows a proof by induction, in a similar spirit as in [38], but with more generic results. In particular, here the (approximate) filtering distribution is the marginalized version of the one in [38] and is constituted by a mixture in the numerator of the importance weights (see [32] for an explanation). In OAPF the proposal density can be any mixture $\psi_t(\mathbf{x}_t)$ fulfilling the standard regularity conditions described above, hence in the denominator of the importance weights, a second mixture appears. Theorem 2 is here the main result, and is supported by Lemmas 1 and 2 which we present first.

Lemma 1 *We have that*

$$\mathbb{E}[\hat{Z}_t|\mathcal{A}_{t-1}] = \sum_{m=1}^M w_{t-1}^{(m)} g(\mathbf{y}_t|\mathbf{x}_{t-1}^{(m)}). \quad (21)$$

Proof:

$$\mathbb{E}[\hat{Z}_t|\mathcal{A}_{t-1}] = \mathbb{E}\left[\frac{1}{M} \sum_{m=1}^M \tilde{w}_t^{(m)}|\mathcal{A}_{t-1}\right] \quad (22)$$

$$= \mathbb{E}\left[\frac{1}{M} \sum_{m=1}^M \frac{g(\mathbf{y}_t|\mathbf{x}_t^{(m)}) \sum_{j=1}^M w_{t-1}^{(j)} f(\mathbf{x}_t^{(m)}|\mathbf{x}_{t-1}^{(j)})}{\psi(\mathbf{x}_t^{(m)})}|\mathcal{A}_{t-1}\right] \quad (23)$$

$$= \frac{1}{M} \sum_{m=1}^M \mathbb{E}\left[\frac{g(\mathbf{y}_t|\mathbf{x}_t^{(m)}) \sum_{j=1}^M w_{t-1}^{(j)} f(\mathbf{x}_t^{(m)}|\mathbf{x}_{t-1}^{(j)})}{\psi(\mathbf{x}_t^{(m)})}|\mathcal{A}_{t-1}\right]. \quad (24)$$

Now, since given \mathcal{A}_{t-1} the particles at time t are conditionally independent with pdf $\psi_t(\mathbf{x}_t)$, then we have that the integrals within (24) are identical:

$$\mathbb{E}[\hat{Z}_t|\mathcal{A}_{t-1}] = \int \frac{g(\mathbf{y}_t|\mathbf{x}_t) \sum_{j=1}^M w_{t-1}^{(j)} f(\mathbf{x}_t|\mathbf{x}_{t-1}^{(j)})}{\psi(\mathbf{x}_t)} \psi(\mathbf{x}_t) d\mathbf{x}_t \quad (25)$$

$$= \int g(\mathbf{y}_t|\mathbf{x}_t) \sum_{j=1}^M w_{t-1}^{(j)} f(\mathbf{x}_t|\mathbf{x}_{t-1}^{(j)}) d\mathbf{x}_t \quad (26)$$

$$= \sum_{j=1}^M w_{t-1}^{(j)} \int g(\mathbf{y}_t, \mathbf{x}_t|\mathbf{x}_{t-1}^{(j)}) d\mathbf{x}_t \quad (27)$$

$$= \sum_{j=1}^M w_{t-1}^{(j)} g(\mathbf{y}_t|\mathbf{x}_{t-1}^{(j)}). \quad (28)$$

□

Lemma 2 For any $h \in \{1, \dots, t-1\}$ we have that

$$\mathbb{E}[\hat{Z}_{t-h:t}|\mathcal{A}_{t-h-1}] = \sum_{m=1}^M w_{t-h-1}^{(m)} g(\mathbf{y}_{t-h:t}|\mathbf{x}_{t-h-1}^{(m)}) \quad (29)$$

Proof: We follow a proof by induction. First, note that (29) is true for $h = 0$ due to Lemma 1. Then, we assume that (29) holds for a given h and we will prove that it then holds for $h + 1$. Let us start developing the left-hand side of (29) for $h + 1$ by first noting that $\hat{Z}_{t-h-1:t} = \hat{Z}_{t-h:t} \hat{Z}_{t-h-1}$. Then,

$$\mathbb{E}[\hat{Z}_{t-h-1:t}|\mathcal{A}_{t-h-2}] = \mathbb{E}\left[\mathbb{E}[\hat{Z}_{t-h:t}|\mathcal{A}_{t-h-1}] \hat{Z}_{t-h-1}|\mathcal{A}_{t-h-2}\right] \quad (30)$$

$$= \mathbb{E}\left[\left[\sum_{m=1}^M g(\mathbf{y}_{t-h:t}|\mathbf{x}_{t-h-1}^{(m)}) w_{t-h-1}^{(m)}\right] \hat{Z}_{t-h-1}|\mathcal{A}_{t-h-2}\right] \quad (31)$$

$$(32)$$

where we have simply substituted Eq. (29) that we assume to hold for h . Next,

$$\mathbb{E}[\hat{Z}_{t-h-1:t}|\mathcal{A}_{t-h-2}] = \mathbb{E}\left[\left[\sum_{m=1}^M g(\mathbf{y}_{t-h:t}|\mathbf{x}_{t-h-1}^{(m)}) \frac{\tilde{w}_{t-h-1}^{(m)}}{\sum_{j=1}^M \tilde{w}_{t-h-1}^{(j)}}\right] \frac{1}{M} \sum_{j=1}^M \tilde{w}_{t-h-1}^{(j)}|\mathcal{A}_{t-h-2}\right] \quad (33)$$

$$= \mathbb{E}\left[\frac{1}{M} \sum_{m=1}^M g(\mathbf{y}_{t-h:t}|\mathbf{x}_{t-h-1}^{(m)}) \frac{g(\mathbf{y}_{t-h-1}|\mathbf{x}_{t-h-1}^{(m)}) \sum_{j=1}^M w_{t-h-2}^{(j)} f(\mathbf{x}_{t-h-1}^{(m)}|\mathbf{x}_{t-h-2}^{(j)})}{\psi_{t-h-1}(\mathbf{x}_{t-h-1}^{(m)})}|\mathcal{A}_{t-h-2}\right] \quad (34)$$

$$= \frac{1}{M} \sum_{m=1}^M \mathbb{E}\left[g(\mathbf{y}_{t-h:t}|\mathbf{x}_{t-h-1}^{(m)}) \frac{g(\mathbf{y}_{t-h-1}|\mathbf{x}_{t-h-1}^{(m)}) \sum_{j=1}^M w_{t-h-2}^{(j)} f(\mathbf{x}_{t-h-1}^{(m)}|\mathbf{x}_{t-h-2}^{(j)})}{\psi(\mathbf{x}_{t-h-1}^{(m)})}|\mathcal{A}_{t-h-2}\right] \quad (35)$$

where we have substituted with the importance weights $\tilde{w}_{t-h-1}^{(m)}$ of Eq. 7 of the manuscript. Since, given \mathcal{A}_{t-h-2} , the particles at time t are conditionally independent with pdf $\psi_{t-h-1}(\mathbf{x}_{t-h-1})$, all M expectations are identical:

$$\mathbb{E}[\hat{Z}_{t-h-1:t}|\mathcal{A}_{t-h-2}] = \int g(\mathbf{y}_{t-h:t}|\mathbf{x}_{t-h-1}) \frac{g(\mathbf{y}_{t-h-1}|\mathbf{x}_{t-h-1}) \sum_{j=1}^M w_{t-h-2}^{(j)} f(\mathbf{x}_{t-h-1}|\mathbf{x}_{t-h-2}^{(j)})}{\psi(\mathbf{x}_{t-h-1})} \psi(\mathbf{x}_{t-h-1}) d\mathbf{x}_{t-h-1} \quad (36)$$

$$= \int g(\mathbf{y}_{t-h:t}|\mathbf{x}_{t-h-1}) g(\mathbf{y}_{t-h-1}|\mathbf{x}_{t-h-1}) \sum_{j=1}^M w_{t-h-2}^{(j)} f(\mathbf{x}_{t-h-1}|\mathbf{x}_{t-h-2}^{(j)}) d\mathbf{x}_{t-h-1} \quad (37)$$

$$= \int g(\mathbf{y}_{t-h-1:t}|\mathbf{x}_{t-h-1}) \sum_{j=1}^M w_{t-h-2}^{(j)} f(\mathbf{x}_{t-h-1}|\mathbf{x}_{t-h-2}^{(j)}) d\mathbf{x}_{t-h-1} \quad (38)$$

Step (37) to (38) is justified since $\mathbf{y}_{t-h:t} \perp\!\!\!\perp \mathbf{y}_{t-h-1}|\mathbf{x}_{t-h-1}$, so we can replace $g(\mathbf{y}_{t-h:t}|\mathbf{x}_{t-h-1})$ in 37 with $g(\mathbf{y}_{t-h:t}|\mathbf{y}_{t-h-1}, \mathbf{x}_{t-h-1})$ and then $g(\mathbf{y}_{t-h-1:t}|\mathbf{x}_{t-h-1}) = g(\mathbf{y}_{t-h:t}|\mathbf{x}_{t-h-1})g(\mathbf{y}_{t-h-1}|\mathbf{x}_{t-h-1})$ follows by the chain rule. Next,

$$= \sum_{j=1}^M w_{t-h-2}^{(j)} \int g(\mathbf{y}_{t-h-1:t}, \mathbf{x}_{t-h-1}|\mathbf{x}_{t-h-2}^{(j)}) d\mathbf{x}_{t-h-1} \quad (39)$$

$$= \sum_{j=1}^M w_{t-h-2}^{(j)} g(\mathbf{y}_{t-h-1:t}|\mathbf{x}_{t-h-2}^{(j)}) \quad (40)$$

$$(41)$$

which is the right-hand side of (29). □

Theorem 2 *The OAPF estimator of the normalizing constant is unbiased, i.e., $\mathbb{E}[\hat{Z}_{1:t}] = p(\mathbf{y}_{1:t})$.*

Proof: The unbiasedness is a consequence of Lemma 2 with $h = t - 1$. \square

Now we look at the variance of the normalizing constant estimators. First, we establish a superiority in performance (i.e., equal or less variance) of the OAPF importance weights. This result is also used below to prove the convergence of the estimators by standard results in particle filtering.

Let us particularize importance weights in OAPF for the case with $K = M$ as

$$\tilde{w}_t^{(m)} = \frac{g(\mathbf{y}_t | \mathbf{x}_t^{(m)}) \sum_{i=1}^M w_{t-1}^{(i)} f(\mathbf{x}_t^{(m)} | \mathbf{x}_{t-1}^{(i)})}{\sum_{i=1}^M \lambda_t^{(i)} q_t^{(i)}(\mathbf{x}_t^{(m)} | \bar{\mathbf{x}}_{t-1}^{(i)})}. \quad (42)$$

We also consider the generalized APF weights given by

$$\tilde{v}_t^{(m)} = \frac{g(\mathbf{y}_t | \mathbf{x}_t^{(m)}) w_{t-1}^{(m)} f(\mathbf{x}_t^{(m)} | \mathbf{x}_{t-1}^{(m)})}{\lambda_t^{(m)} q_t^{(m)}(\mathbf{x}_t^{(m)} | \bar{\mathbf{x}}_{t-1}^{(m)})}. \quad (43)$$

These are generalized in the sense that the concrete APF described in the main paper is obtained by setting $\lambda_t^{(m)} \propto w_{t-1}^{(m)} g(\mathbf{y}_t | \boldsymbol{\mu}_t^{(m)})$ and propagating particles with transition kernels $f(\cdot)$, thus our following discussion holds for any choice of $\lambda_t^{(m)}$.

Lemma 3 *The conditional variance of \hat{Z}_t^{OAPF} using the OAPF weights in (42) is always less or equal than the same estimator \hat{Z}_t^{APF} using the APF weights in (43).*

Proof: First, note that $\tilde{v}_t^{(m)}$ can be interpreted as an importance weight in an extended space on \mathbf{x}_t and the auxiliary variable m (see for instance [32, Section 3.1] and [30, 84]). Next, $\tilde{w}_t^{(m)}$ can be interpreted as a version of $\tilde{v}_t^{(m)}$ where both in the numerator (approximate filtering pdf) and denominator (proposal pdf), the auxiliary variable has been marginalized. Then, the variance inequality for each importance weight holds from the application of the variance decomposition lemma (also known as law of total variance). This proof generalizes the result in [32] for any set of mixture weights $\{\lambda_t^{(m)}\}_{m=1}^M$, with $\sum_{j=1}^M \lambda_t^{(j)} = 1$ and $\lambda_t^{(m)} \geq 0$, for all m . Finally, since both \hat{Z}_t^{OAPF} and \hat{Z}_t^{APF} are constructed as the average of the OAPF and APF weights, respectively, the conditional variance of \hat{Z}_t^{OAPF} is necessarily upper-bounded by that of \hat{Z}_t^{APF} . \square

We now address the consistency of the normalizing constant, $\hat{Z}_{1:t}$, and the self-normalized IS (SNIS) estimator $\hat{I}(h_t) = \sum_{m=1}^M w_t^{(m)} h_t(\mathbf{x}_t^{(m)})$.

Corollary 1 *The OAPF estimator of the normalizing constant $\hat{Z}_{1:t}$ and the SNIS estimator $\hat{I}(h_t)$ are consistent, i.e., $\lim_{M \rightarrow \infty} \hat{Z}_{1:t} = p(\mathbf{y}_{1:t})$ and $\lim_{M \rightarrow \infty} \hat{I}(h_t) = I(h_t)$ a.s. (almost surely) for a finite t .*

Proof: The consistency of $\hat{Z}_{1:t}$ is a consequence of its unbiasedness, proved in Theorem 2, and the variance inequality in Lemma 3, which ensures the variance convergence to zero a.s. when $N \rightarrow \infty$ since the APF, which upper-bounds its variance, is also consistent [36, Section 3.6]. A similar argumentation can be done for the SNIS estimator $\hat{I}(h_t)$. Note that the SNIS estimator can be re-expressed as $\hat{I}(h_t) = \sum_{m=1}^M \frac{\tilde{w}_t^{(m)}}{M \hat{Z}_t} h_t(\mathbf{x}_t^{(m)}) = \frac{1}{M} \sum_{m=1}^M \frac{\tilde{w}_t^{(m)}}{\hat{Z}_t} h_t(\mathbf{x}_t^{(m)})$. Since \hat{Z}_t is a consistent estimator of $p(\mathbf{y}_t | \mathbf{y}_{1:t-1})$, the denominator converges to $p(\mathbf{y}_t | \mathbf{y}_{1:t-1})$ while the numerator converges to $p(\mathbf{y}_t | \mathbf{y}_{1:t-1}) I(h_t)$, when $N \rightarrow \infty$. Therefore, the ratio converges to $I(h_t)$ a.s. \square

A.2 Additional Experiments and Results

A.2.1 Experiment 1

We provide all necessary parameters to reproduce Figure 1 in the main paper. We recall that in this toy example we do the Bayesian recursion from $t - 1$ to t with $M = 4$ particles. In Figure 1(a), we have set the particles $\{\bar{\mathbf{x}}_{t-1}^{(m)}\}_{m=1}^{M=4} = \{2, 2.5, 3, 3.5\}$, the normalized weights $\{3/10, 3/10, 1/5, 1/5\}$, likelihood centered at 3, and $\sigma_{\text{lik}} = 0.8$, and $\sigma_{\text{kern}} = 0.5$.

In Figure 1(b), $\{\bar{\mathbf{x}}_{t-1}^{(m)}\}_{m=1}^{M=4} = \{2, 2.5, 5, 5.5\}$, the normalized weights are $\{7/22, 1/11, 1/2, 1/11\}$, the likelihood is

centered at 3.5, and $\sigma_{\text{lik}} = 1.2$, and $\sigma_{\text{kern}} = 0.5$. The proposals of all algorithms are then calculated as:

$$\sum_{m=1}^4 \lambda_t^{(m)} f(\mathbf{x}_t | \bar{\mathbf{x}}_{t-1}^{(m)}), \quad (44)$$

where the mixture weights $\lambda_t^{(m)}$ for BPF are $w_{t-1}^{(m)}$, for APF are $\propto w_{t-1}^{(m)} g(\mathbf{y}_t | \boldsymbol{\mu}_t^{(m)})$, for IAPF $\propto g(\mathbf{y}_t | \boldsymbol{\mu}_t^{(m)}) \sum_{m=1}^M w_{t-1}^{(m)} f(\boldsymbol{\mu}_t^{(m)} | \bar{\mathbf{x}}_{t-1}^{(m)}) / \sum_{m=1}^M f(\boldsymbol{\mu}_t^{(m)} | \bar{\mathbf{x}}_{t-1}^{(m)})$ and finally for OAPF they are the solution to the NNLS optimization problem.

As specified in the main paper and can be seen from 44, we used transition kernels as proposal kernels for OAPF. Moreover, we used the centers of the transition kernels $\boldsymbol{\mu}_t^{(m)}$ as evaluation points, which in this case they correspond to the resampled particles $\{\bar{\mathbf{x}}_{t-1}^{(m)}\}_{m=1}^M$.

A.2.2 Experiment 2

We provide the equations of the linear dynamical model (LDM) and full results for Experiment 2 in the main paper. The model is given by

$$p(\mathbf{x}_0) = \mathcal{N}_{\mathbf{x}_0}(\mathbf{m}_0, \boldsymbol{\Sigma}_0) \quad (45)$$

$$f(\mathbf{x}_t | \mathbf{x}_{t-1}) = \mathcal{N}_{\mathbf{x}_t}(\mathbf{A}\mathbf{x}_{t-1} + \mathbf{c}, \mathbf{R}) \quad (46)$$

$$g(\mathbf{y}_t | \mathbf{x}_t) = \mathcal{N}_{\mathbf{y}_t}(\mathbf{C}\mathbf{x}_t + \mathbf{g}, \mathbf{Q}). \quad (47)$$

The posterior filtering distribution can be computed in closed form via the Kalman filter:

$$p(\mathbf{x}_t | \mathbf{y}_{1:t}) = \mathcal{N}_{\mathbf{x}_t}(\boldsymbol{\mu}_t, \boldsymbol{\Sigma}_t) \quad (48)$$

$$\boldsymbol{\mu}_t = \bar{\boldsymbol{\mu}}_t + \mathbf{K}(\mathbf{y}_t - \mathbf{C}\bar{\boldsymbol{\mu}}_t - \mathbf{g}) \quad (49)$$

$$\boldsymbol{\Sigma}_t = (\mathbf{I} - \mathbf{K}\mathbf{C})\bar{\boldsymbol{\Sigma}}_t \quad (50)$$

$$\bar{\boldsymbol{\mu}}_t = \mathbf{A}\boldsymbol{\mu}_{t-1} + \mathbf{c} \quad (51)$$

$$\bar{\boldsymbol{\Sigma}}_t = \mathbf{A}\boldsymbol{\Sigma}_{t-1}\mathbf{A}^\top + \mathbf{R} \quad (52)$$

$$\mathbf{K} = \bar{\boldsymbol{\Sigma}}_t \mathbf{C}^\top (\mathbf{C}\bar{\boldsymbol{\Sigma}}_t \mathbf{C}^\top + \mathbf{Q})^{-1}. \quad (53)$$

Moreover, $p(\mathbf{y}_{1:t})$ can also be computed in closed form from $p(\mathbf{y}_t | \mathbf{y}_{1:t-1})$. For numerical stability, one computes $\log p(\mathbf{y}_{1:t})$ and $\log p(\mathbf{y}_t | \mathbf{y}_{1:t-1})$, which are given by:

$$\log p(\mathbf{y}_{1:t}) = \log p(\mathbf{y}_1) + \sum_{\tau=2}^t \log p(\mathbf{y}_\tau | \mathbf{y}_{1:\tau-1}) \quad (54)$$

$$\log p(\mathbf{y}_\tau | \mathbf{y}_{1:\tau-1}) = -\frac{1}{2} [\log(|\mathbf{C}\bar{\boldsymbol{\Sigma}}_\tau \mathbf{C}^\top + \mathbf{Q}|) + (\mathbf{y}_\tau - \mathbf{C}\bar{\boldsymbol{\mu}}_\tau - \mathbf{g})^\top (\mathbf{C}\bar{\boldsymbol{\Sigma}}_\tau \mathbf{C}^\top + \mathbf{Q})^{-1} (\mathbf{y}_\tau - \mathbf{C}\bar{\boldsymbol{\mu}}_\tau - \mathbf{g}) + d_{\mathbf{y}_\tau} \ln(2\pi)] \quad (55)$$

$$\log p(\mathbf{y}_1) = -\frac{1}{2} [\log(|\mathbf{C}\boldsymbol{\Sigma}_0 \mathbf{C}^\top + \mathbf{Q}|) + (\mathbf{y}_1 - \mathbf{C}\bar{\boldsymbol{\mu}}_1 - \mathbf{g})^\top (\mathbf{C}\boldsymbol{\Sigma}_0 \mathbf{C}^\top + \mathbf{Q})^{-1} (\mathbf{y}_1 - \mathbf{C}\bar{\boldsymbol{\mu}}_1 - \mathbf{g}) + d_{\mathbf{y}_1} \ln(2\pi)]. \quad (56)$$

We set $\mathbf{R} = 5\mathbf{I}$ and $\mathbf{Q} = 2.5\mathbf{I}$. In this setting, the kernels overlap and the observations are very informative. The setting is particularly advantageous for IAPF, and hence it is more difficult to beat its performance. Moreover, $\mathbf{A} = \frac{1}{2}\mathbf{I}$ and $\mathbf{C} = \frac{1}{2}\mathbf{I}$. For $d_{\mathbf{x}_t} = 2$, then $\mathbf{c} = \mathbf{g} = (-2, 2)^\top$; for $d_{\mathbf{x}_t} = 5$, then $\mathbf{c} = \mathbf{g} = (-2, 2, -2, 2, -2)^\top$; similarly defined for $d_{\mathbf{x}_t} = 10$. The results for all $d_{\mathbf{x}_t}$ are shown in Table 4. We recall that in this experiment, OAPF ran with $\mathbf{K} = \mathbf{5}$, $\mathbf{E} = \mathbf{5}$. This implies large computational savings with respect to the IAPF (or similarly to any other algorithm which uses the full mixture in the denominator of the importance weights).

A.2.3 Experiment 3

In this experiment, we have used the standard parameters for the Lorenz model given by $(s, r, b) = (10, 28, 2.667)$. We set transition and observation noise as independent standard normally distributed random variables. In Figure 3, we show visually, as stated in the main paper, how a small change in Δt can lead to very different trajectories of \mathbf{x}_t . The sensitivity to Δt , to the initialization, and even to the parameters (s, r, b) , jointly with the strong non-linearity of the generated trajectories, make the Lorenz model particularly challenging.

Table 4: Full results for Experiment 2 in main paper. The Table shows normalized MSE as defined in the paper, with standard errors over 100 Monte Carlo runs. Recall that whenever $d_{\mathbf{x}_t} \in \{2, 5\}$ then $M = 100$ and when $d_{\mathbf{x}_t} = 10$ then $M = 1000$.

Method	$d_{\mathbf{x}_t} = 2$	$d_{\mathbf{x}_t} = 5$	$d_{\mathbf{x}_t} = 10$
BPF	$3.19 \cdot 10^{-7} \pm 3.14 \cdot 10^{-8}$	$5.09 \cdot 10^{-7} \pm 4.40 \cdot 10^{-8}$	$1.539 \cdot 10^{-7} \pm 1.267 \cdot 10^{-8}$
APF	$3.51 \cdot 10^{-7} \pm 3.88 \cdot 10^{-8}$	$4.68 \cdot 10^{-7} \pm 4.49 \cdot 10^{-8}$	$1.333 \cdot 10^{-7} \pm 1.224 \cdot 10^{-8}$
IAPF	$2.15 \cdot 10^{-7} \pm 2.25 \cdot 10^{-8}$	$1.63 \cdot 10^{-7} \pm 1.58 \cdot 10^{-8}$	$6.330 \cdot 10^{-8} \pm 6.204 \cdot 10^{-9}$
OAPF	$1.35 \cdot 10^{-7} \pm 1.23 \cdot 10^{-8}$	$9.67 \cdot 10^{-8} \pm 9.03 \cdot 10^{-9}$	$4.771 \cdot 10^{-8} \pm 5.329 \cdot 10^{-9}$

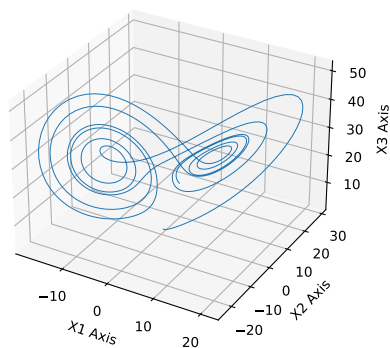
Table 5: Results with additional parameters for Experiment 4. Note that when $d_{\mathbf{x}_t} = 10$ then $M = 1000$. Averaged ESS and standard errors over 100 Monte Carlo runs.

Method	$d_{\mathbf{x}_t} = 2$	$d_{\mathbf{x}_t} = 5$	$d_{\mathbf{x}_t} = 10$
BPF	63.5 ± 0.2	33.5 ± 0.2	108.7 ± 0.8
APF	63.5 ± 0.2	34.5 ± 0.2	107.2 ± 1.0
IAPF	73.0 ± 0.1	44.9 ± 0.2	203.5 ± 0.9
OAPF	88.3 ± 0.2	63.5 ± 0.2	366.2 ± 1.8

A.2.4 Experiment 4

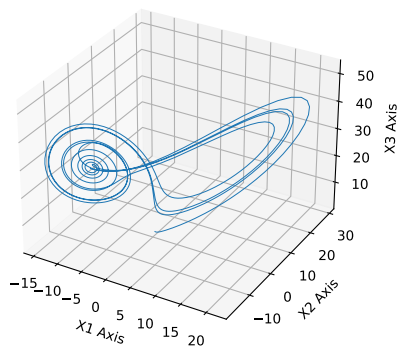
In this experiment, we have used a challenging multivariate stochastic volatility model, which is common in related works (see for instance [66]). Additional results with parameters $\mathbf{m} = \mathbf{0}$, $\mathbf{U}_0 = \mathbf{I}$, $\mathbf{U} = \mathbf{I}$, $\phi = \frac{1}{2}\mathbf{1}$ are shown in Table 5.

Lorenz 63 noiseless trajectory



(a)

Lorenz 63 noiseless trajectory



(b)

Figure 3: In this figure, we show the noiseless versions of a trajectory for $\Delta t = 0.01$ (a) and $\Delta t = 0.008$ (b) to emphasize how different trajectories can be in a Lorenz 63 model even with small parameter changes. Note that particle filters will have to deal with both transition noise and observation noise.

References

- [1] Simo Särkkä. *Bayesian filtering and smoothing*, volume 3. Cambridge University Press, 2013.
- [2] Marcel Hirt and Petros Dellaportas. Scalable bayesian learning for state space models using variational inference with smc samplers. volume 89 of *Proceedings of Machine Learning Research*, pages 76–86. PMLR, 16–18 Apr 2019.
- [3] Arnaud Doucet, Nando De Freitas, and Neil Gordon. An introduction to sequential monte carlo methods. In *Sequential Monte Carlo methods in practice*, pages 3–14. Springer, 2001.
- [4] M Sanjeev Arulampalam, Simon Maskell, Neil Gordon, and Tim Clapp. A tutorial on particle filters for online nonlinear/non-gaussian bayesian tracking. *IEEE Transactions on signal processing*, 50(2):174–188, 2002.
- [5] Petar M Djuric, Jayesh H Kotecha, Jianqui Zhang, Yufei Huang, Tadesse Ghirmai, Mónica F Bugallo, and Joaquin Miguez. Particle filtering. *IEEE signal processing magazine*, 20(5):19–38, 2003.
- [6] Pierre Del Moral. Feynman-kac formulae. In *Feynman-Kac Formulae*, pages 47–93. Springer, 2004.
- [7] Sebastian Thrun. Particle filters in robotics. In *Proceedings of the Eighteenth conference on Uncertainty in artificial intelligence*, pages 511–518. Morgan Kaufmann Publishers Inc., 2002.
- [8] Nikos Vlassis, Bas Terwijn, and Ben Krose. Auxiliary particle filter robot localization from high-dimensional sensor observations. In *Proceedings 2002 IEEE International Conference on Robotics and Automation (Cat. No. 02CH37292)*, volume 1, pages 7–12. IEEE, 2002.
- [9] Cody Kwok, Dieter Fox, and Marina Meila. Real-time particle filters. In *Advances in neural information processing systems*, pages 1081–1088, 2003.
- [10] Ananta Adhi Wardhana, Evan Clearesta, Augie Widyotriatmo, et al. Mobile robot localization using modified particle filter. In *2013 3rd International Conference on Instrumentation Control and Automation (ICA)*, pages 161–164. IEEE, 2013.
- [11] Katja Nummiaro, Esther Koller-Meier, and Luc Van Gool. An adaptive color-based particle filter. *Image and vision computing*, 21(1):99–110, 2003.
- [12] Guangyu Zhu, Dawei Liang, Yang Liu, Qingming Huang, and Wen Gao. Improving particle filter with support vector regression for efficient visual tracking. In *IEEE International Conference on Image Processing 2005*, volume 2, pages II–422. IEEE, 2005.
- [13] Hedibert F Lopes and Ruey S Tsay. Particle filters and bayesian inference in financial econometrics. *Journal of Forecasting*, 30(1):168–209, 2011.
- [14] Maria Paula Rios and Hedibert Freitas Lopes. The extended liu and west filter: Parameter learning in markov switching stochastic volatility models. In *State-Space Models*, pages 23–61. Springer, 2013.
- [15] MJ Keeling and P Rohani. Stochastic dynamics. *Modeling Infectious Diseases in Humans and Animals*, pages 190–230, 2007.
- [16] Daniel M Sheinson, Jarad Niemi, and Wendy Meiring. Comparison of the performance of particle filter algorithms applied to tracking of a disease epidemic. *Mathematical biosciences*, 255:21–32, 2014.
- [17] Peter Dawson, Ralph Gailis, and Alaster Meehan. Detecting disease outbreaks using a combined bayesian network and particle filter approach. *Journal of theoretical biology*, 370:171–183, 2015.
- [18] Alexandre Piché, Valentin Thomas, Cyril Ibrahim, Yoshua Bengio, and Chris Pal. Probabilistic planning with sequential monte carlo methods. In *International Conference on Learning Representations*, 2019.
- [19] Chris J. Maddison, Dieterich Lawson, George Tucker, Nicolas Heess, Arnaud Doucet, Andriy Mnih, and Yee Whye Teh. Particle value functions. In *5th International Conference on Learning Representations, ICLR 2017, Toulon, France, April 24-26, 2017, Workshop Track Proceedings*. OpenReview.net, 2017.
- [20] Yunbo Wang, Bo Liu, Jiajun Wu, Yuke Zhu, Simon S Du, Li Fei-Fei, and Joshua B Tenenbaum. Dualsmc: Tunneling differentiable filtering and planning under continuous pomdps. *Proceedings of the Twenty-Ninth International Joint Conference on Artificial Intelligence, IJCAI-20*, 2020.
- [21] Dieterich Lawson, George Tucker, Christian A Naesseth, Chris J Maddison, Ryan P Adams, and Yee Whye Teh. Twisted variational sequential monte carlo. In *Third workshop on Bayesian Deep Learning (NeurIPS)*, 2018.
- [22] Tuan Anh Le, Maximilian Igl, Tom Rainforth, Tom Jin, and Frank Wood. Auto-encoding sequential monte carlo. In *6th International Conference on Learning Representations, ICLR 2018, Vancouver, BC, Canada, April 30 - May 3, 2018, Conference Track Proceedings*. OpenReview.net, 2018.

- [23] Antonio Khalil Moretti, Zizhao Wang, Luhuan Wu, and Itsik Pe'er. Smoothing nonlinear variational objectives with sequential monte carlo. In *Deep Generative Models for Highly Structured Data, ICLR 2019 Workshop, New Orleans, Louisiana, United States, May 6, 2019*. OpenReview.net, 2019.
- [24] Shixiang Shane Gu, Zoubin Ghahramani, and Richard E Turner. Neural adaptive sequential monte carlo. In *Advances in neural information processing systems*, pages 2629–2637, 2015.
- [25] Christian Naesseth, Scott Linderman, Rajesh Ranganath, and David Blei. Variational sequential monte carlo. volume 84 of *Proceedings of Machine Learning Research*, pages 968–977, Playa Blanca, Lanzarote, Canary Islands, 09–11 Apr 2018. PMLR.
- [26] Xiao Ma, Péter Karkus, David Hsu, and Wee Sun Lee. Particle filter recurrent neural networks. In *The Thirty-Fourth AAAI Conference on Artificial Intelligence, AAAI 2020*, pages 5101–5108. AAAI Press, 2020.
- [27] Yunpeng Li and Mark Coates. Particle filtering with invertible particle flow. *IEEE Transactions on Signal Processing*, 65(15):4102–4116, 2017.
- [28] Nicholas Metropolis and Stanislaw Ulam. The monte carlo method. *Journal of the American statistical association*, 44(247):335–341, 1949.
- [29] Neil J Gordon, David J Salmond, and Adrian FM Smith. Novel approach to nonlinear/non-gaussian bayesian state estimation. In *IEE proceedings F (radar and signal processing)*, volume 140, pages 107–113. IET, 1993.
- [30] Michael K Pitt and Neil Shephard. Filtering via simulation: Auxiliary particle filters. *Journal of the American statistical association*, 94(446):590–599, 1999.
- [31] Simon Godsill and Tim Clapp. Improvement strategies for monte carlo particle filters. In *Sequential Monte Carlo methods in practice*, pages 139–158. Springer, 2001.
- [32] Mike Klaas, Nando de Freitas, and Arnaud Doucet. Toward practical n2 monte carlo: the marginal particle filter. In *Proceedings of the Twenty-First Conference Annual Conference on Uncertainty in Artificial Intelligence (UAI-05)*, pages 308–315, Arlington, Virginia, 2005. AUAI Press.
- [33] Art B Owen. Monte carlo theory, methods and examples. *Monte Carlo Theory, Methods and Examples*. Art Owen, 2013.
- [34] Mateu Sbert, Vlastimil Havran, and Laszlo Szirmay-Kalos. Multiple importance sampling revisited: breaking the bounds. *EURASIP Journal on Advances in Signal Processing*, 2018(1):15, 2018.
- [35] Víctor Elvira, Luca Martino, David Luengo, Mónica F Bugallo, et al. Generalized multiple importance sampling. *Statistical Science*, 34(1):129–155, 2019.
- [36] Arnaud Doucet and Adam M Johansen. A tutorial on particle filtering and smoothing: Fifteen years later. *Handbook of nonlinear filtering*, 12(656-704):3, 2009.
- [37] Víctor Elvira, Luca Martino, Mónica F Bugallo, and Petar M Djurić. In search for improved auxiliary particle filters. In *2018 26th European Signal Processing Conference (EUSIPCO)*, pages 1637–1641. IEEE, 2018.
- [38] Michael K Pitt, Ralph dos Santos Silva, Paolo Giordani, and Robert Kohn. On some properties of markov chain monte carlo simulation methods based on the particle filter. *Journal of Econometrics*, 171(2):134–151, 2012.
- [39] Evan Archer, Il Memming Park, Lars Buesing, John Cunningham, and Liam Paninski. Black box variational inference for state space models. *arXiv preprint arXiv:1511.07367*, 2015.
- [40] David M Blei, Alp Kucukelbir, and Jon D McAuliffe. Variational inference: A review for statisticians. *Journal of the American statistical Association*, 112(518):859–877, 2017.
- [41] Adji Bousso Dieng, Dustin Tran, Rajesh Ranganath, John Paisley, and David Blei. Variational inference via χ upper bound minimization. In *Advances in Neural Information Processing Systems*, pages 2732–2741, 2017.
- [42] Victor Elvira, Luca Martino, Monica F Bugallo, and Petar M Djuric. Elucidating the auxiliary particle filter via multiple importance sampling [lecture notes]. *IEEE Signal Processing Magazine*, 36(6):145–152, 2019.
- [43] Tiancheng Li, Miodrag Bolic, and Petar M Djuric. Resampling methods for particle filtering: classification, implementation, and strategies. *IEEE Signal processing magazine*, 32(3):70–86, 2015.
- [44] Adam M Johansen and Arnaud Doucet. A note on auxiliary particle filters. *Statistics & Probability Letters*, 78(12):1498–1504, 2008.
- [45] Nick Whiteley and Adam M Johansen. Auxiliary particle filtering: recent developments. *Bayesian time series models*. Cambridge University Press, Cambridge, 2011.
- [46] Eric Veach and Leonidas J Guibas. Optimally combining sampling techniques for monte carlo rendering. In *Proceedings of the 22nd annual conference on Computer graphics and interactive techniques*, pages 419–428, 1995.

- [47] Monica F Bugallo, Victor Elvira, Luca Martino, David Luengo, Joaquin Miguez, and Petar M Djuric. Adaptive importance sampling: The past, the present, and the future. *IEEE Signal Processing Magazine*, 34(4):60–79, 2017.
- [48] J. S. Liu. *Monte Carlo Strategies in Scientific Computing*. Springer, 2004.
- [49] Ernest K Ryu and Stephen P Boyd. Adaptive importance sampling via stochastic convex programming. *arXiv preprint arXiv:1412.4845*, 2014.
- [50] Joaquín Míguez. On the performance of nonlinear importance samplers and population Monte Carlo schemes. In *2017 22nd International Conference on Digital Signal Processing (DSP)*, pages 1–5. IEEE, 2017.
- [51] W. Feller. *An Introduction to Probability and Its Applications*, volume II of *Wiley Publication in Mathematical Statistics*. Wiley India Pvt. Limited, 1966.
- [52] H. W. Sorenson and D. L. Alspach. Recursive Bayesian estimation using Gaussian sums. *Automatica*, pages 465–479, 1971.
- [53] Jayesh H Kotecha and Petar M Djuric. Gaussian sum particle filtering. *IEEE Transactions on signal processing*, 51(10):2602–2612, 2003.
- [54] Christophe Andrieu, Arnaud Doucet, and Roman Holenstein. Particle markov chain monte carlo methods. *Journal of the Royal Statistical Society: Series B (Statistical Methodology)*, 72(3):269–342, 2010.
- [55] Nikolas Kantas, Arnaud Doucet, Sumeetpal S Singh, Jan Maciejowski, Nicolas Chopin, et al. On particle methods for parameter estimation in state-space models. *Statistical science*, 30(3):328–351, 2015.
- [56] David Luengo, Luca Martino, Mónica Bugallo, Víctor Elvira, and Simo Särkkä. A survey of monte carlo methods for parameter estimation. *EURASIP Journal on Advances in Signal Processing*, 2020(1):1–62, 2020.
- [57] Arnaud Doucet, Simon Godsill, and Christophe Andrieu. On sequential monte carlo sampling methods for bayesian filtering. *Statistics and computing*, 10(3):197–208, 2000.
- [58] Martin Slawski and Matthias Hein. Sparse recovery by thresholded non-negative least squares. In *Advances in Neural Information Processing Systems*, pages 1926–1934, 2011.
- [59] Martin Slawski, Matthias Hein, et al. Non-negative least squares for high-dimensional linear models: Consistency and sparse recovery without regularization. *Electronic Journal of Statistics*, 7:3004–3056, 2013.
- [60] Nicolai Meinshausen et al. Sign-constrained least squares estimation for high-dimensional regression. *Electronic Journal of Statistics*, 7:1607–1631, 2013.
- [61] Charles L Lawson and Richard J Hanson. *Solving least squares problems*. SIAM, 1995.
- [62] Rasmus Bro and Sijmen De Jong. A fast non-negativity-constrained least squares algorithm. *Journal of Chemometrics: A Journal of the Chemometrics Society*, 11(5):393–401, 1997.
- [63] Nicolas Nadisic, Arnaud Vandaele, Nicolas Gillis, and Jeremy E Cohen. Exact sparse nonnegative least squares. In *ICASSP 2020-2020 IEEE International Conference on Acoustics, Speech and Signal Processing (ICASSP)*, pages 5395–5399. IEEE, 2020.
- [64] Yuancheng Luo and Ramani Duraiswami. Efficient parallel nonnegative least squares on multicore architectures. *SIAM Journal on Scientific Computing*, 33(5):2848–2863, 2011.
- [65] Volodymyr Kysenko, Karl Rupp, Oleksandr Marchenko, Siegfried Selberherr, and Anatoly Anisimov. Gpu-accelerated non-negative matrix factorization for text mining. In *International Conference on Application of Natural Language to Information Systems*, pages 158–163. Springer, 2012.
- [66] Pieralberto Guarniero. *The Iterated Auxiliary Particle Filter and Applications to State Space Models and Diffusion Processes*. PhD thesis, University of Warwick, 2017.
- [67] Jeremy Heng, Adrian N Bishop, George Deligiannidis, Arnaud Doucet, et al. Controlled sequential monte carlo. *Annals of Statistics*, 48(5):2904–2929, 2020.
- [68] Ömer Deniz Akyildiz and Joaquín Míguez. Nudging the particle filter. *Statistics and Computing*, 30(2):305–330, 2020.
- [69] Julien Cornebise, Eric Moulines, and Jimmy Olsson. Adaptive sequential monte carlo by means of mixture of experts. *Statistics and Computing*, 24(3):317–337, 2014.
- [70] Joel Kronander and Thomas B Schön. Robust auxiliary particle filters using multiple importance sampling. In *2014 IEEE Workshop on Statistical Signal Processing (SSP)*, pages 268–271. IEEE, 2014.
- [71] E. N. Lorenz. Deterministic nonperiodic flow. *Journal of Atmospheric Sciences*, 20(2):130–141, 1963.

- [72] Edward Ott, Brian R Hunt, Istvan Szunyogh, Aleksey V Zimin, Eric J Kostelich, Matteo Corazza, Eugenia Kalnay, DJ Patil, and James A Yorke. A local ensemble kalman filter for atmospheric data assimilation. *Tellus A: Dynamic Meteorology and Oceanography*, 56(5):415–428, 2004.
- [73] Hoong C Yeong, Ryne T Beeson, N Sri Namachchivaya, and Nicolas Perkowski. Particle filters with nudging in multiscale chaotic systems: With application to the lorenzâ€™96 atmospheric model. *Journal of Nonlinear Science*, pages 1–34, 2020.
- [74] Pieralberto Guarniero, Adam M Johansen, and Anthony Lee. The iterated auxiliary particle filter. *Journal of the American Statistical Association*, 112(520):1636–1647, 2017.
- [75] David JC MacKay and David JC Mac Kay. *Information theory, inference and learning algorithms*. Cambridge university press, 2003.
- [76] Sebastian M. Schmon, Arnaud Doucet, and George Deligiannidis. Bernoulli race particle filters. volume 89 of *Proceedings of Machine Learning Research*, pages 2350–2358. PMLR, 16–18 Apr 2019.
- [77] Ayman Boustati, Ömer Deniz Akyildiz, Theodoros Damoulas, and Adam Johansen. Generalized bayesian filtering via sequential monte carlo. In *Advances in neural information processing systems*, 2020.
- [78] Rudolph Emil Kalman et al. A new approach to linear filtering and prediction problems. *Journal of basic Engineering*, 82(1):35–45, 1960.
- [79] Víctor Elvira, Joaquín Míguez, and Petar M Djurić. Adapting the number of particles in sequential monte carlo methods through an online scheme for convergence assessment. *IEEE Transactions on Signal Processing*, 65(7):1781–1794, 2017.
- [80] Andrew G Wilson and Zoubin Ghahramani. Copula processes. In *Advances in Neural Information Processing Systems*, pages 2460–2468, 2010.
- [81] Jonathan R Stroud, Nicholas G Polson, and Peter Müller. Practical filtering for stochastic volatility models. *State space and unobserved components models*, pages 236–247, 2004.
- [82] Paul Fearnhead. Using random quasi-monte-carlo within particle filters, with application to financial time series. *Journal of Computational and Graphical Statistics*, 14(4):751–769, 2005.
- [83] Siddhartha Chib, Yasuhiro Omori, and Manabu Asai. Multivariate stochastic volatility. In *Handbook of Financial Time Series*, pages 365–400. Springer, 2009.
- [84] Simon Godsill. Particle filtering: the first 25 years and beyond. In *ICASSP 2019-2019 IEEE International Conference on Acoustics, Speech and Signal Processing (ICASSP)*, pages 7760–7764. IEEE, 2019.